Research Square

Preprints are preliminary reports that have not undergone peer review.
They should not be considered conclusive, used to inform clinical practice,
or referenced by the media as validated information.

Exosomal miRNA balance links estrogen receptor signaling to CDK4/6 inhibitor outcomes

Maria Angeles Domínguez-Cejudo

mdcejudo-ibis@us.es

Instituto de Biomedicina de Sevilla

Raquel Chapresto-Garzón

Instituto de Biomedicina de Sevilla

Ana Gil-Torralvo

Hospital Universitario Virgen del Rocío

Maria Angeles Castilla

Hospital Universitario Virgen del Rocío

Begoña Vieites

Hospital Universitario Virgen del Rocío

Maria Luisa Valdivia

Instituto de Biomedicina de Sevilla

Mónica Cejuela

Hospital Universitario Virgen del Rocío

Marta Benavent

Hospital Universitario Virgen del Rocío

Alejandro Falcón-Gonzalez

Hospital Universitario Virgen del Rocío

Marta Amerigo-Gongora

Hospital Universitario Virgen del Rocío

Rocío Perez

Hospital Universitario Virgen del Rocío

Alberto Moreno

Hospital Universitario Virgen del Rocío

Manuel Ruiz-Borrego

Hospital Universitario Virgen del Rocío

Sonia Molina-Pinelo

Instituto de Biomedicina de Sevilla

Javier Salvador-Bofill

Hospital Universitario Virgen del Rocío

Article

Keywords: Metastatic breast cancer, CDK4/6 inhibitors, Exosomal microRNAs, miR-155-5p, miR-143-3p, Liquid biopsy, Endocrine resistance, Tumor–host interactions

Posted Date: May 19th, 2026

DOI: https://doi.org/10.21203/rs.3.rs-9042970/v1

License: This work is licensed under a Creative Commons Attribution 4.0 International License. Read Full License

Additional Declarations: Competing interest reported. AG-T declares honoraria from Novartis, AstraZeneca, Daiichi, and Pfizer; travel and accommodation support from Novartis, Pfizer, and Daiichi; and advisory roles with Daiichi and AstraZeneca. She also holds a patent with Roche. MC declares financial relationships with Novartis, Pfizer, and Lilly, including grants for patient care improvement programs, participation in advisory boards, and company-sponsored travel and accommodation. MB declares consulting and advisory roles with Pfizer and Novartis, and travel and accommodation support from Pfizer and Novartis. AF declares honoraria from Roche, Pfizer, Novartis, Lilly, Menarini, AstraZeneca, MSD, Daiichi, Gilead, Dr. Reddy, and Grünenthal; travel and accommodation support from Novartis, Daiichi, Gilead, and Roche; and advisory roles with Roche, Pfizer, Menarini, AstraZeneca, and MSD. MA-G has received funding for speaker bureau from Kyowa Kirin and Grünenthal. AM declares honoraria from Novartis; and travel and accommodation support from Novartis and Pfizer; MR-B declares honoraria from Pfizer, Gilead, and AstraZeneca; speaker honoraria from Daiichi Sankyo, AstraZeneca, and Pierre-Fabre; and advisory roles with Pfizer, Gilead, and AstraZeneca. JS-B declares honoraria from Roche, Pfizer, Novartis, Lilly, AstraZeneca, MSD, Daiichi, and Gilead; travel and accommodation support from Novartis and Roche; and advisory roles with Lilly and Novartis. All other authors declare no potential conflicts of interest.

Abstract

Background:

Cyclin-dependent kinase 4/6 inhibitors (CDK4/6i) combined with endocrine therapy have transformed the treatment landscape of estrogen receptor–positive (ER+) metastatic breast cancer. However, therapeutic benefit remains heterogeneous, and clinically applicable biomarkers capable of capturing endocrine sensitivity states and predicting treatment durability are lacking. Increasing evidence suggests that inflammatory signaling programs interact with ER activity, yet circulating biomarkers reflecting this regulatory interface remain poorly defined.

Experimental Design:

We performed exploratory profiling of plasma-derived exosomal microRNAs using microarray analysis in a discovery cohort of ER+ metastatic breast cancer patients initiating first-line CDK4/6i therapy. Differentially expressed miRNAs between hormone-sensitive and hormone-resistant patients were identified and subjected to pathway enrichment analyses. miR-155-5p was prioritized for validation in an independent cohort (n = 69) using quantitative PCR. Given the functional antagonism between miR-155-5p and miR-143-3p in inflammatory and metabolic regulatory pathways, a miR-155-5p/miR-143-3p expression ratio was constructed to capture this regulatory balance. Associations with progression-free survival, overall survival, time-dependent predictive performance, and estrogen receptor expression were evaluated.

Results:

Thirty-seven exosomal miRNAs distinguished hormone-sensitive and hormone-resistant patients and converged on pathways related to inflammation, metabolic adaptation, and endocrine resistance. Elevated exosomal miR-155-5p levels were associated with shorter PFS in the validation cohort (HR 1.89, p = 0.03). The miR-155-5p/miR-143-3p ratio further refined prognostic stratification, identifying patients with significantly different PFS outcomes (HR 1.88, p = 0.02). Time-dependent ROC analysis demonstrated stable discriminatory performance across follow-up (AUC 0.64–0.69 at 12–24 months). Importantly, higher ratios correlated inversely with ER expression ($\rho = -0.22$, p = 0.038), linking this circulating miRNA balance to endocrine regulatory states.

Conclusions:

A circulating exosomal miRNA regulatory balance between miR-155-5p and miR-143-3p identifies ER+ metastatic breast cancer patients with inferior outcomes under CDK4/6 inhibition. These findings support the concept that exosomal miRNA networks can capture the inflammatory–endocrine regulatory

interface underlying heterogeneous endocrine sensitivity. Circulating miRNA balances may therefore represent minimally invasive biomarkers to refine patient stratification and inform risk-adapted therapeutic strategies in ER+ metastatic breast cancer.

INTRODUCTION

Estrogen receptor–positive (ER+) / HER2-negative metastatic breast cancer (MBC) represents the most prevalent subtype of advanced breast cancer and remains a leading cause of cancer-related mortality in women worldwide (1). The introduction of cyclin-dependent kinase 4/6 inhibitors (CDK4/6i) in combination with endocrine therapy (ET) has transformed first-line management, substantially prolonging progression-free and overall survival across multiple trials (2–8). Despite these advances, treatment response remains highly heterogeneous, and most patients ultimately develop resistance. In clinical practice, ER + MBC encompasses distinct endocrine sensitivity states at treatment initiation. Patients may present with either endocrine-sensitive or endocrine-resistant disease, which is associated with more aggressive clinical behavior, faster disease progression, and inferior outcomes under CDK4/6 inhibition (9, 10). The biological determinants underlying this heterogeneity remain poorly understood.

Emerging evidence indicates that ER signaling itself is closely associated with inflammatory and immune regulatory pathways in breast cancer. High ER expression has been related with reduced immune infiltration and suppression of inflammatory programs, including interferon signaling, antigen presentation, and tumor inflammation signatures (11–13). These observations suggest that ER signaling and tumor-associated inflammation exist in a dynamic regulatory balance that may influence treatment response, yet the molecular mediators linking these processes remain to be defined. As a result, robust biomarkers capable of capturing this inflammatory–endocrine interplay and predicting the duration of benefit from CDK4/6 inhibitors are still lacking.

Current biomarker efforts have primarily focused on tumor-intrinsic alterations, including ESR1 mutations, RB1 loss, cyclin D activation, alterations in the PI3K/AKT/mTOR pathway, and transcriptomic signatures, yet their predictive value in clinical practice is limited (14–18). Liquid biopsy approaches, particularly circulating tumor DNA (ctDNA), have improved detection of acquired ESR1 mutations, but have not yielded reliable predictors of CDK4/6i benefit (19–21). In contrast, exosomal microRNAs (miRNAs) have emerged as promising biomarkers (22). These small extracellular vesicles circulate stably in plasma. Their cargo is selectively enriched rather than randomly packaged and carry miRNAs that mirror dynamic biological signals from tumors and peripheral immune cells (23). Numerous studies have shown that exosomal miRNA profiles differentiate tumor states, predict recurrence, and capture inflammatory and metabolic cues (22). This makes them an ideal substrate for biomarker discovery in settings where resistance involves complex, multi-cellular processes.

Given the diversity of miRNA species and their multi-target regulatory functions, a comprehensive profiling approach is essential to identify candidate biomarkers linked to CDK4/6i response. High-throughput microarray analysis of exosomal miRNAs enables unbiased discovery of miRNAs whose

expression correlates with clinical outcomes, facilitating hypothesis generation and subsequent targeted validation. In this study, we first performed an exploratory microarray analysis of plasma exosomal miRNAs in patients with ER + MBC initiating CDK4/6i treatment to identify candidate biomarkers of progression. Among the miRNAs identified from this analysis, miR-155-5p emerged as a strong candidate. miR-155-5p is a well-established regulator of inflammatory signalling pathways, including NF-κB and STAT3, and is involved in metabolic rewiring and immune modulation in cancer (24, 25). Notably, miR-155-5p operates within a regulatory axis with miR-143-3p, a miRNA with opposing tumor-suppressive and anti-glycolytic functions, suggesting that the balance between these miRNAs may reflect the inflammatory and metabolic state of the tumor–host environment (26, 27). We therefore performed targeted validation of miR-155-5p expression and investigated the clinical relevance of the miR-155-5p/miR-143-3p balance in relation to survival outcomes, time-dependent predictive performance, and its association with ER signaling. Together, our findings support the concept that exosomal miRNAs can function as integrative biomarkers reflecting tumor–host interactions, and identify the miR-155-5p/miR-143-3p regulatory balance as a novel indicator of inflammatory–metabolic state and clinical outcome in ER + MBC treated with CDK4/6i.

MATERIALS & METHODS

Study design and patient population

This was a retrospective translational study using prospectively collected plasma samples from patients diagnosed with locally advanced or ER + MBC who received CDK4/6i as a first-line therapy at the Hospital Virgen del Rocío between November 2018 and December 2023 (Fig. 1). Those who received at least one cycle of treatment with abemaciclib, palbociclib, or ribociclib plus ET and were followed up for at least 1 year were selected. Patients who had received previous therapy for MBC were excluded. All premenopausal patients received parallel ovarian function suppression. Disease progression was determined by the attending clinician based on radiology, pathology, and clinical assessment. Data regarding histologic type, hormone receptors, Ki67 expression, and HER2 status were collected from pathology reports. Tumor stage and other clinical data, including treatment information, were obtained from electronic medical records.

Endocrine resistance was established following the fourth ESO-ESMO International consensus recommendations. Primary endocrine resistance was defined as a relapse during the first 2 years of adjuvant ET. Secondary endocrine resistance was defined as a relapse while on adjuvant ET, but after the first 2 years, or relapse within 12 months of completing adjuvant ET. The study procedures were approved by the Coordinating Committee on Biomedical Research Ethics of Andalucía (0920-N20). All patients provided written informed consent.

Plasma sample processing and isolation of exosomes

Peripheral blood was collected from each patient before receiving treatment in BD Vacutainer® tubes (BD Biosciences, USA). Plasma samples were obtained by centrifugation at 3,000 rpm for 20 min at RT and stored at − 80 ∘C for subsequent experiments.

3 or 5 mL of processed plasma was used as starting material for isolating exosomes from each sample incorporated in the discovery or validation phase, respectively. Exosomes were isolated from plasma by ultracentrifugation as previously described (28). Briefly, plasma was diluted (1:20) with PBS and centrifuged at 15.000 × g for 40 minutes to remove cells and debris. Then, the resultant supernatant was filtered through a 0.22-mm filter (Millipore, USA), transferred to a sterile ultracentrifuge tube, and then centrifuged at 120.000 x g for 3h at 4ºC (Beckman Optima XE-90, Beckman Coulter, USA). For exosome purification, the pellets were washed in a large volume of PBS and centrifuged again under the same conditions. Following this step, the pellets containing the exosomes were collected and resuspended in 50 uL of filtrated PBS for subsequent studies.

Characterization of isolated exosomes (TEM, WB, NanoSight)

Morphological analysis of exosomes was conducted using transmission electron microscopy (TEM) at the Electron Microscopy Service of the Research, Technology and Innovation Centre (CITIUS, University of Seville). Samples were prepared using a standard negative staining protocol with 2% uranyl acetate, providing optimal contrast for ultrastructural visualization. Sample imaging was performed with a Zeiss Libra 120 transmission electron microscope operated at an acceleration voltage of 120 kV. Images were captured using a 2-megapixel SSCCD camera, allowing high-resolution documentation of vesicle morphology.

Exosomal proteins were extracted using RIPA buffer and quantified by BCA colorimetric method. Western blot analysis of exosome-related proteins was performed following standard procedures. Briefly, about 35 µg of protein was separated on 8% SDS-PAGE gels and transferred onto PVDF membranes. After blocking with 5% non-fat dry milk in TBS-T, membranes were incubated with primary antibodies against CD81 (M30; Thermo Fisher Scientific, #10630D), tumor susceptibility gene 101 (TSG101; Santa Cruz, SC-7964), and Calnexin (AF18; Santa Cruz, SC-23954). Detection was performed using HRP-conjugated secondary antibodies and the Amersham™ ECL Select™ Western Blotting Detection Reagent (Cytiva, #RPN2235) according to the manufacturer's protocol.

The size distribution of nanoparticles in exosome preparations was analyzed by the LM10 nanoparticle tracking system (NanoSight) equipped with a blue laser (405 nm) for real-time classification of the vesicles.

RNA extraction

Plasma-derived exosomal preparations were resuspended in 50 µL of PBS prior to extraction. Total RNA, including small RNA species such as microRNAs, was isolated using the *mirVana™ miRNA Isolation Kit*

(Thermo Fisher Scientific), following the manufacturer's protocol. To ensure the efficiency and integrity of the RNA isolation process, 1 µL of synthetic RNA control was added to each sample using the *RNA Spike-In Kit for RT* (Qiagen, USA), following the manufacturer's instructions.

MicroArray analysis

Gene Chip microarray analysis was performed by Affymetrix® FlashTag™ Biotin HSR RNA Labeling Kits (Genisphere, LLC, Hatfield, PA, USA). Briefly, total RNA was tailed by poly(A), incubated at 37 ºC for 15 min, end-labelled by the FlashTag™ sequence (incubated at 25ºC for 30 min) containing biotin through the use of peroxidase-antiperoxidase enzyme and T4 DNA Ligase. End-labelled miRNA was hybridised to the GeneChip® miRNA 4.0 arrays (Affymetrix Inc., Santa Clara, CA, USA) for 16–18 hours at 48ºC and 60 rpm. After hybridisation, Gene Chips were stained and washed by the GeneChip® Fluidics Station 450 (Affymetrix Inc.) and scanned using a GeneChip® Array scanner 3000 7 G (Affymetrix Inc.). Expression intensity results were recorded from the scanned images using Affymetrix Command Console software version 1.1.

Raw data were automatically extracted using the Affymetrix data extraction protocol in the Affymetrix GeneChip® Command Console® Software (AGCC). CEL file import, normalization using the RMA+DABG algorithm, and export of the results were all performed using Transcriptome Analysis Console Software 4.0.2. After log2 translation of the normalized signal intensities, the data were compared. A comparative analysis between the hormone-sensitive (HS) and the hormone-resistant (HR) samples was carried out using fold-change and an independent *t*-test, in which the null hypothesis was 'there is no difference between the groups'. Hierarchical clustering was performed using complete linkage and Euclidean distance as a measure of similarity for the differentially expressed miRNAs. Statistical tests and visualization of differentially expressed miRNAs were conducted according to the R statistical language v. 4.4.1. The Gene Expression Omnibus accession number for the microarray data is GSE315252.

miRNA targets prediction and functional enrichment analysis

Predicted target genes of the differentially expressed miRNAs were obtained using the *TAC Software* version 4.0.2 (Thermo Fisher Scientific, USA). These predicted targets were then subjected to functional enrichment analysis to explore their biological significance. Pathway annotation was performed using the *Database for Annotation, Visualization, and Integrated Discovery (DAVID*, https://davidbioinformatics.nih.gov/), followed by classification with the *Kyoto Encyclopedia of Genes and Genomes (KEGG)* database. Significantly enriched pathways were defined as those with a false discovery rate (FDR) < 0.05 and fold enrichment > 2. Visualization of enrichment results was conducted in *R* v4.4.1 using the ggplot2 package.

Validation by qPCR

Quantification of exosomal miR-155-5p and miR-143-3p expression was performed by qPCR. Briefly, 2 µL of total RNA were reverse transcribed using the TaqMan® Advanced miRNA cDNA Synthesis Kit (Applied Biosystems, Thermo Fisher Scientific, UK), following the manufacturer's instructions. Real-time PCR was conducted using the TaqMan® Advanced miRNA Assay specific for hsa-miR-155-5p (Assay ID: 477983_mir) and has-miR-143-3p (Assay ID: 477912_mir) together with the TaqMan® Fast Advanced Master Mix, on a ViiA™ 7 Real-Time PCR System (Applied Biosystems). The mature sequences are UUAAUGCUAAUCGUGAUAGGGGU (MIMAT0000646) and UGAGAUGAAGCACUGUAGCUC (MIMAT0000435), as annotated in miRBase v22. Normalization was performed using hsa-miR-103a-3p (Assay ID: 478286_mir), a commonly used endogenous control in plasma miRNA profiling, which shares the same TaqMan® Advanced platform. Its mature sequence is AGCAGCAUUGUACAGGGCUAUGA (MIMAT0000101). All reactions were run in triplicate, and relative expression was calculated using the $2^{-\Delta\Delta Ct}$ method (29), with expression levels normalized to both endogenous and spike-in controls.

Statistical analysis

Statistical analyses were performed using R software (version 4.4.2). Continuous variables were summarized as medians and ranges, while categorical variables were reported as frequencies and percentages. The primary endpoint was progression-free survival (PFS). Overall survival (OS) was analyzed as a secondary endpoint.

Group comparisons between two independent variables were performed using the Wilcoxon rank-sum test for continuous data and the chi-square or Fisher’s exact test for categorical variables, as appropriate. Correlations between continuous variables were assessed using Spearman’s rank correlation coefficient.

Survival outcomes, PFS and overall survival OS, were estimated using the Kaplan–Meier method and compared with the log-rank test. Hazard ratios (HRs) and 95% confidence intervals (CIs) were calculated using Cox proportional hazards regression models.

To evaluate the time-dependent discriminatory performance of circulating biomarkers, receiver operating characteristic (ROC) analyses were performed using the timeROC R package, which estimates the area under the curve (AUC) at prespecified time points while accounting for censoring in survival data. AUC values and corresponding confidence intervals were calculated at 12, 18, and 24 months.

All tests were two-sided, and a p-value < 0.05 was considered statistically significant.

RESULTS

Characteristics of the study population

A total of 95 patients with ER+ metastatic breast cancer treated with first-line CDK4/6i were included in the study and distributed into discovery (n = 26) and validation (n = 69) cohorts. The median age of the

overall population was 55 years, with a balanced distribution of premenopausal and postmenopausal patients. Most tumors were ductal carcinomas and belonged to the luminal B subtype. Approximately 31% of patients met criteria for endocrine resistance at treatment initiation. CDK4/6i use and concomitant ET were similarly distributed between cohorts. No significant differences were observed between the discovery and validation cohorts across baseline clinicopathologic characteristics, supporting their comparability for downstream analyses (Table 1).

Table 1. Characteristics of the study population

	All n=95 (%)	Discovery cohort n=26 (%)	Validation cohort n=69 (%)	*p value*
Mean Age (years)	55 (51.8-56.9)	51 (47.8-58.9)	55 (51.8-57.7)	0.72
Menopausal status				
Premenopausal	35 (36.84)	13 (50)	22 (31.89)	0.15
Postmenopausal	60 (63.16)	13 (50)	47 (68.11)	
Histopathologic status				
DC	68 (71.58)	20 (76.92)	48 (69.56)	
LC	15 (15.79)	4 (15.38)	11 (15.95)	0.93
Others	12 (12.63)	2 (7.7)	10 (14.49)	
Luminal subtype				
Luminal A	32 (33.68)	7 (26.92)	25 (36.23)	0.39
Luminal B	63 (66.32)	19 (73.08)	44 (63.77)	
Endocrine resistant				
Yes	30 (31.58)	12 (46.15)	15 (21.74)	0.08
No	65 (68.42)	14 (53.85)	54 (78.26)	
Tumor grade				
Grade 1	19 (20)	6 (23.08)	13 (18.85)	0.44
Grade 2	29 (30.53)	8 (30.77)	21 (30.43)	
Grade 3	22 (23.16)	8 (30.77)	14 (20.29)	
Unknown	25 (26.31)	4 (15.38)	21 (30.43)	
CDK4/6i				
Abemaciclib	29 (30.53)	10 (38.46)	19 (27.54)	0.5
Palbociclib	37 (38.94)	10 (38.46)	27 (39.13)	
Ribociclib	29 (30.53)	6 (23.08)	23 (33.33)	
Concomitant ET				
AI*	65 (68.42)	19 (73.08)	46 (66.66)	0.63
Fulvestrant	30 (31.58)	7 (26.92)	23 (33.34)	

DC: Ductal carcinoma; LC: lobular carcinoma; ET: Endocrine therapy; AI: Aromatase inhibitor.

* AI includes: letrozole and anastrozole.

Plasma-derived exosomes isolation and characterization

To determine the presence of circulating exosomes in ER+ metastatic breast cancer patients, we characterized extracellular vesicles isolated from plasma samples. Exosomes were isolated using ultracentrifugation and subsequently analyzed by TEM. TEM imaging revealed multiple isolated vesicles with a characteristic **rounded, cup-shaped morphology** and a **double membrane structure** (Figure S1A). Western blot analysis confirmed the identity of exosomes by detecting the presence of **TSG101** and **CD81**, two well-established exosomal markers. As expected, the negative control **Calnexin** was not detected, confirming the purity of the isolated vesicles (Figure S1B). Using nanoparticle tracking analysis, a well-established technique for measuring size distribution of molecules and particles in the submicron region, further demonstrated that the vesicle sizes ranged from **70 to 200 nm**, consistent with previously reported exosomal size distributions (Figure S1C). Collectively, these findings confirm the successful isolation and characterization of plasma-derived exosomes from ER+ MBC patients.

Identification of Candidate Biomarkers in the Exploratory Cohort

To identify circulating exosomal miRNAs associated with response to CDK4/6i, we performed miRNA microarray profiling (Genechip™ miRNA 4.0 Array, Affymetrix, USA) on exosomes isolated from 26 mBC patients (HR: n = 12 HS: n = 14) prior to therapy initiation. Following quality control assessment, 22 samples (HR = 9, HS = 13) were normalized and included in the differential expression analysis (Figure 2A).

Unsupervised Principal Component Analysis of all small non-coding RNAs revealed that the miRNA expression profiles clearly separated HR and HS patient samples, indicating distinct molecular signatures (Figure 2B). Differential expression analysis using an ANOVA model ($p < 0.05$, fold change ≥ 1.5) identified 37 miRNAs that were significantly dysregulated between HR and HS patients (Table 2). Of these, 26 miRNAs were downregulated, while 11 miRNAs were upregulated in HR patients (Figure 2C&D). Unsupervised hierarchical clustering analysis of the top 20 differentially expressed miRNAs generated a heatmap dendrogram, revealing a clear separation of HR and HS patient samples, indicating the predictive value of these miRNAs in ER+ MBC patients (Figure 2E).

Table 2. Diferentially expressed miRNAs.

Transcript ID	Fold Change	P-value	Assay ID (Array design)
hsa-miR-216a-5p	1,6	0,0001	20500475
hsa-mir-3178	-1,72	0,0002	20536289
hsa-miR-6846-5p	-1,83	0,0007	20525653
hsa-miR-551b-5p	-1,64	0,0008	20504289
hsa-mir-6078	-1,61	0,0010	20537251
hsa-miR-6511a-5p	-1,94	0,0015	20525023
hsa-miR-7154-5p	-1,67	0,0015	20526868
hsa-mir-4744	-1,55	0,0015	20536982
hsa-miR-155-5p	1,86	0,0017	20501083
hsa-miR-4529-3p	-2,65	0,0023	20518930
hsa-miR-1285-3p	1,53	0,0024	20506813
hsa-miR-5681a	1,67	0,0024	20522012
hsa-miR-4283	-1,71	0,0031	20517743
hsa-miR-6735-5p	-1,7	0,0037	20525432
hsa-mir-6800	1,56	0,0055	20537544
hsa-mir-4741	-1,67	0,0056	20536979
hsa-miR-4314	-1,76	0,0058	20517696
hsa-miR-4690-5p	-1,66	0,0058	20519498
hsa-miR-6886-5p	-1,66	0,0070	20525733
hsa-miR-4764-3p	1,53	0,0077	20519638
hsa-miR-4655-5p	-1,66	0,0080	20519439
hsa-miR-3936	-1,73	0,0092	20518624
hsa-miR-4775	1,51	0,0117	20519654
hsa-miR-2277-5p	-1,81	0,0124	20512261
hsa-miR-1225-5p	-1,54	0,0136	20506763
hsa-miR-6514-5p	-1,59	0,0137	20525029
hsa-miR-1184	-1,93	0,0152	20506716
hsa-miR-378b	-1,59	0,0170	20515536

hsa-miR-6800-5p	1,82	0,0170	20525561
hsa-miR-6789-5p	1,73	0,0174	20525539
hsa-mir-6886	-1,79	0,0225	20537632
hsa-miR-4492	-1,66	0,0236	20518887
hsa-mir-5703	1,64	0,0251	20537225
hsa-mir-6727	-1,73	0,0255	20537470
hsa-miR-6068	3,14	0,0279	20523000
hsa-miR-4665-5p	-1,5	0,0365	20519457
hsa-miR-4669	-1,54	0,0423	20519467

Functional Significance of Dysregulated miRNAs

To elucidate the biological significance of the differentially expressed miRNAs, we identified their predicted target genes using Transcriptome Analysis Console Software 4.0.2. The resulting gene list was then subjected to gene enrichment analysis using the DAVID database. Pathway enrichment analysis was performed using **KEGG annotation**, with significantly enriched pathways defined as those with **fold enrichment > 2 and a false discovery rate (FDR) < 0.05**. The KEGG pathway enrichment analysis revealed that **upregulated miRNAs in HR patients** were significantly associated with key oncogenic and metabolic pathways, including the **FOXO signaling pathway, TNF signaling pathway, endocrine resistance, stem cell regulatory pathways, and the Hippo signaling pathway** (Figure 3A). These pathways are strongly linked to **cell survival, metabolic adaptation, and drug resistance,** which are critical hallmarks of therapy-resistant in breast cancer. Conversely, **downregulated miRNAs in HR patients** were primarily associated with **ferroptosis, adherens junctions, cell cycle regulation, cellular senescence, and the TGF-beta signaling pathway** (Figure 3B). These pathways are **crucial for maintaining cellular homeostasis, restricting unchecked proliferation, and promoting programmed cell death mechanisms**, suggesting a potential loss of tumor-suppressive mechanisms in HR patients, favoring increased tumor **progression**, immune evasion, and therapy resistance.

To further investigate the role of individual miRNAs within these pathways, we analyzed the percentage of genes associated with each miRNA across the enriched signaling pathways (Figure 3C). This analysis revealed that among the upregulated miRNAs, miR-155-5p emerged as a dominant regulator, displaying extensive enrichment with multiple oncogenic pathways, supporting its potential role in endocrine resistance and tumor progression**.** In contrast, the downregulated miRNAs in HR patients showed a more disperse distribution across pathways.

Together, these findings indicate that the **dysregulated miRNA landscape in HR patients impacts multiple oncogenic and regulatory pathways, reinforcing a more aggressive and therapy-resistant phenotype**. Notably, the **dominance of miR-155-5p across multiple pathways underscores its potential**

as a key driver of endocrine resistance, making it a compelling candidate for further investigation as a biomarker in ER+ MBC.

Validation of miR-155-5p as biomarker for Predicting Sensitivity to CDK4/6i therapy

To validate the predictive performance of miR-155-5p, we enrolled an independent cohort of 69 patients with similar clinicopathological characteristic as the discovery cohort (Table1). Exosomal miR-155-5p expression was quantified, and its association with clinical outcomes was evaluated in terms of PFS and OS.

Patients were stratified into high- and low-expression groups using the median expression value to minimize overfitting and allow balanced group comparison. Kaplan-Meier survival analysis revealed that patients with high miR-155-5p expression exhibited significantly shorter PFS compared to those with low expression (HR = 1.89, 95% CI: 1.05–3.37, *p- val* = 0.033) (Figure 4A). The median PFS for high-expression patients was 24.9 months, whereas the median for the low-expression group was 44.18 (Log-rank test, *p-val* = 0.03), further supporting the adverse prognostic role of miR-155-5p in endocrine-resistant MBC. Regarding OS, a consistent but non-statistically significant trend was observed (Figure 4B). Patients with high miR-155-5p expression showed shorter median OS compared with those with low expression (49.6 vs 66.3 months; log-rank p = 0.077), with a hazard ratio of 1.88 (95% CI: 0.90–3.80, p = 0.082). Although not reaching statistical significance, the concordant direction and magnitude of effect support a potential adverse prognostic impact of elevated miR-155-5p expression.

Collectively, these findings strongly support the clinical utility of exosomal miR-155-5p as a biomarker, reinforcing its potential to identify patients with poorer outcomes despite CDK4/6 inhibitor therapy.

miR-155-5p is associated with inflammation and treatment response

Emerging evidence indicates that the interplay between miR-155-5p and miR-143-3p plays a key role in regulating cellular metabolism and inflammation, particularly by modulating glycolytic flux and immune responses in the tumor microenvironment (26,30). In this regulatory axis, miR-155 has been shown to promote glycolysis and inflammatory signaling, while miR-143 exerts opposing, tumor-suppressive effects. Given this functional antagonism, we explored whether dominance of either miRNA was associated with treatment outcomes.

To investigate this, we first calculated the miR-155-5p/miR-143-3p expression ratio and stratified the patients based on miRNA dominance: miR-155-dominant (ratio > 1) versus miR-143-dominant (ratio < 1; SupTable3). Kaplan-Meier survival analysis revealed that miR-143-dominant patients had significantly longer PFS compared to their miR-155-dominant counterparts (Figure 5A). The mean PFS was 46.8months for miR-143-dominant patients, while it was reduced to 23.1 months in the miR-155-dominant group (log-rank, p- value = 0.02). Cox regression analysis confirmed that miR-155 dominance was associated with a 1.88-fold increased risk of progression (95% CI: 1.1–2.9, p = 0.02), suggesting reduced therapeutic benefit from CDK4/6 inhibition. Consistent with PFS findings, OS analysis showed a

similar but non-significant trend toward poorer outcomes in the miR-155-dominant group (HR = 1.67, 95% CI: 0.9–3.2, p = 0.12) (Figure 5B), supporting a sustained adverse prognostic impact of this regulatory imbalance. To further characterize the predictive performance of this inflammatory miRNA axis, time-dependent ROC analysis was performed using the ratio as a continuous variable. The discriminatory accuracy improved over time, with an AUC of 0.64 at 12 months (95% CI: 0.49–0.79), increasing to 0.69 at 18 months (95% CI: 0.56–0.82), and remaining stable at 24 months (AUC 0.69, 95% CI: 0.57–0.80), indicating stable prognostic performance during follow-up (Supplementary Figure 2).

Given the established interplay between inflammatory signaling and ER activity, we next investigated whether this miRNA-defined inflammatory balance was associated with ER expression. Correlation analysis revealed a modest but significant inverse relationship between ER levels and the miR-155-5p/miR-143-3p ratio (Spearman ρ = −0.22, p = 0.038) (Figure 5C). Consistently, ER levels were significantly reduced in miR-155-dominant tumors compared with miR-143-dominant cases (Wilcoxon p = 0.0027) (Figure 5D).

DISCUSSION

In this study, we identify a plasma-derived exosomal miRNA regulatory balance between miR-155-5p and miR-143-3p as a clinically relevant predictor of outcomes in patients with ER + MBC treated with CDK4/6 therapy. Beyond the prognostic impact of miR-155-5p alone, our data demonstrate that the relative dominance of miR-155-5p over its counter-regulatory partner miR-143-3p captures a broader biological state characterized by metabolic adaptation and reduced ER activity. The convergence between miRNA balance and ER expression supports the concept that this exosomal miRNA axis reflects an integrated regulatory interface linking inflammatory signaling programs with endocrine pathway activity. To our knowledge, this study provides the first clinical evidence that an exosomal miRNA regulatory balance can simultaneously capture inflammatory–metabolic signaling and ER pathway activity while predicting therapeutic outcomes in patients receiving CDK4/6 inhibition.

Our data highlight a key concept relevant to the evolving understanding of CDK4/6 treatment resistance. The identification of miR-155-5p reinforces the idea that the biology driving resistance extends beyond tumor-intrinsic genomic alterations. While ESR1 mutations, RB1 loss, CCND1 amplification and other tumor-centric markers have been extensively explored, they capture only a fraction of the clinical heterogeneity observed in this setting (14–18). The strong association between exosomal miR-155-5p and progression suggests that host–tumor crosstalk, immunometabolic stress, and inflammatory signaling may play a more significant role in modulating CDK4/6i efficacy than previously appreciated. The biological functions of miR-155-5p align closely with these observations. miR-155-5p is a central regulator of inflammatory pathways, including NF-κB and IL-6/STAT3 signaling, both of which have been involved in endocrine resistance, tumor proliferation, and immune remodelling (24, 25). Consistently, different studies in breast cancer models have shown that miR-155 promotes glycolytic reprogramming, supports metabolic adaptation under estrogen deprivation, and drives aggressive phenotypes characterized by increased inflammatory signalling (26, 31, 32). Our findings extend this body of

evidence into the clinical setting, indicating that these miR-155-driven programs may not be merely artifacts of *in vitro* systems but are reflected in the circulating exosomal compartment.

Beyond miR-155-5p, the landscape of differentially expressed exosomal miRNAs identified in the exploratory cohort reinforces the notion that endocrine resistance is governed by coordinated regulatory programs rather than single molecular events. Functional enrichment analysis revealed convergence on pathways related to metabolic adaptation, inflammatory signaling, cell survival, and stress responses, including FOXO, TNF, Hippo, and endocrine resistance pathways. Similar pathway-level convergence of miRNA signatures has been reported in resistant ER+ breast cancer and other solid tumors (27, 33), where distinct miRNA combinations collectively shape adaptive phenotypes. In this context, miR-155-5p may function as a central node within a wider miRNA network that reflects systemic immunometabolic stress, while other dysregulated miRNAs may contribute as complementary players (27). These findings support the value of miRNA profiling approaches for capturing complex resistance biology that may not be apparent from single-gene or mutation-focused analyses.

One novel aspect of this study is the biological contextualization of miR-155-5p within a counter-regulatory miRNA framework rather than as an isolated biomarker. Although miR-143-3p alone did not demonstrate differential expression or independent prognostic value, its inverse relationship with miR-155-5p enabled the definition of a miRNA balance that reflects a broader regulatory state. Importantly, this miR-155-dominant profile was consistently associated with reduced ER expression, supporting the concept that inflammatory and metabolic regulatory programs intersect with endocrine signaling pathways. These findings suggest that exosomal miR-155-5p does not merely act as a marker of aggressive disease but instead functions as part of a coordinated regulatory axis that captures the dynamic interplay between inflammatory signaling, metabolic adaptation, and ER pathway activity.

We also acknowledge limitations. The sample size, while comparable to other translational liquid biopsy studies (19, 34), limits the possibility of subgroup analyses. Functional mechanistic studies were beyond the scope of this clinical investigation but are necessary to dissect how miR-155-driven programs influence tumor proliferation, metabolic rewiring, and immune interactions in the context of CDK4/6i therapy. Moreover, although exosomal miRNAs may originate from both tumor and immune cells, our study design does not distinguish their cellular origin. Future studies integrating spatial and single-cell profiling will be essential to determine the cellular sources and relevance of exosomal miR-155 in the metastatic setting.

In summary, our findings identify exosomal miR-155-5p as a clinically relevant predictor of resistance to CDK4/6 inhibition and support the concept that treatment response is shaped by dynamic regulatory programs rather than static genomic alterations alone. By linking miR-155-5p expression to a coordinated miRNA network and to reduced ER signaling, this study provides clinical evidence for an inflammatory–endocrine regulatory axis that may underlie heterogeneous endocrine sensitivity at treatment initiation. These results highlight the potential of circulating exosomal miRNAs as integrative biomarkers capable of capturing biologically meaningful states that influence therapeutic outcomes. As

CDK4/6i continue to evolve within increasingly complex treatment strategies, biomarkers reflecting this regulatory balance may help refine risk stratification, guide therapeutic sequencing, and inform the development of rational combination approaches aimed at overcoming resistance.

CONCLUSIONS

Circulating exosomal miR-155-5p emerges as a clinically relevant biomarker associated with resistance to CDK4/6 inhibitor–based therapy in ER-positive metastatic breast cancer. Beyond its independent prognostic value, the balance between miR-155-5p and miR-143-3p identifies a regulatory axis linked to treatment outcome and estrogen receptor signaling, supporting an inflammatory–endocrine interplay underlying heterogeneous endocrine sensitivity. These findings underscore the potential of exosomal microRNAs as minimally invasive biomarkers that capture dynamic tumor–host interactions not reflected by tumor-intrinsic alterations alone. These findings may inform future strategies integrating exosomal biomarkers into clinical risk stratification.

LIST OF ABREVATIONS

AI: Aromatase inhibitor

AUC: Area under the curve

CDK4/6i: Cyclin-dependent kinase 4/6 inhibitor

CI: Confidence interval

ER+: Estrogen receptor-positive

ET: Endocrine therapy

HR: Hazard ratio

MBC: Metastatic breast cancer

PFS: Progression-free survival

ROC: Receiver operating characteristic

Declarations

Ethics approval and consent to participate

The study was conducted in accordance with the Declaration of Helsinki and approved by the Coordinating Committee on Biomedical Research Ethics of Andalucía (0920-N20). All patients provided written informed consent for participation, including the collection and analysis of biological samples and associated clinical data.

Competing interests

AG-T declares honoraria from Novartis, AstraZeneca, Daiichi, and Pfizer; travel and accommodation support from Novartis, Pfizer, and Daiichi; and advisory roles with Daiichi and AstraZeneca. She also holds a patent with Roche. MC declares financial relationships with Novartis, Pfizer, and Lilly, including grants for patient care improvement programs, participation in advisory boards, and company-sponsored travel and accommodation. MB declares consulting and advisory roles with Pfizer and Novartis, and travel and accommodation support from Pfizer and Novartis. AF declares honoraria from Roche, Pfizer, Novartis, Lilly, Menarini, AstraZeneca, MSD, Daiichi, Gilead, Dr. Reddy, and Grünenthal; travel and accommodation support from Novartis, Daiichi, Gilead, and Roche; and advisory roles with Roche, Pfizer, Menarini, AstraZeneca, and MSD. MA-G has received funding for speaker bureau from Kyowa Kirin and Grünenthal. AM declares honoraria from Novartis; and travel and accommodation support from Novartis and Pfizer; MR-B declares honoraria from Pfizer, Gilead, and AstraZeneca; speaker honoraria from Daiichi Sankyo, AstraZeneca, and Pierre-Fabre; and advisory roles with Pfizer, Gilead, and AstraZeneca. JS-B declares honoraria from Roche, Pfizer, Novartis, Lilly, AstraZeneca, MSD, Daiichi, and Gilead; travel and accommodation support from Novartis and Roche; and advisory roles with Lilly and Novartis.

All other authors declare no potential conflicts of interest.

Availability of data and materials

The Gene Expression Omnibus accession number for the microarray data is GSE315252. Additional data supporting the findings of this study are available from the corresponding author upon reasonable request.

Acknowledgements & Funding

AG-T was funded by Regional Ministry of Health and Families (RBL-0003-2024). MC was funded by Instituto de Salud Carlos III (ISCIII; Río Hortega Program CM24/00276). SM-P was funded by the Ministry of Health and Social Welfare of Junta de Andalucia (Nicolás Monardes Program RC-0004-20220), ISCIII (PI23/01679) and co-funded by FEDER from Regional Development European Funds (European Union).

The authors thank the patients and their families for their participation. We also acknowledge the support of the Biobank of the Sistema Sanitario Público de Andalucía and the technical assistance provided by the IBiS core facilities.

Authors' contributions

MAD-C, SM-P and JS-B conceived and supervised the study. MAD-C, RC and AG-T performed experimental work and data analysis. JS-B, AG-T, MC, MB, AF-G, MA, RP, AM and MR-B contributed to patient recruitment and clinical data collection. BV performed pathological evaluation. MAD-C wrote the original draft. All authors critically reviewed the manuscript, and approved the final version.

References

1. Bray F, Laversanne M, Sung H, Ferlay J, Siegel RL, Soerjomataram I, et al. Global cancer statistics 2022: GLOBOCAN estimates of incidence and mortality worldwide for 36 cancers in 185 countries. CA Cancer J Clin. 2024;74(3):229–63.
2. Finn RS, Martin M, Rugo HS, Jones S, Im S-A, Gelmon K, et al. Palbociclib and Letrozole in Advanced Breast Cancer. N Engl J Med. 2016;375(20):1925–36.
3. Goetz MP, Toi M, Campone M, Trédan O, Bourayou N, Sohn J, et al. MONARCH 3: Abemaciclib as initial therapy for advanced breast cancer. J Clin Oncol. 2017;35(32):3638–46.
4. Hortobagyi GN, Stemmer SM, Burris HA, Yap Y-S, Sonke GS, Paluch-Shimon S, et al. Ribociclib as First-Line Therapy for HR-Positive, Advanced Breast Cancer. N Engl J Med. 2016;375(18):1738–48.
5. Iwata H, Im SA, Masuda N, Im YH, Inoue K, Rai Y, et al. PALOMA-3: Phase III trial of fulvestrant with or without palbociclib in premenopausal and postmenopausal women with hormone receptor–positive, human epidermal growth factor receptor 2–negative metastatic breast cancer that progressed on prior endocrine th. J Glob Oncol. 2017;3(4):289–303.
6. Sledge GW, Toi M, Neven P, Sohn J, Inoue K, Pivot X, et al. MONARCH 2: Abemaciclib in combination with fulvestrant in women with HR+/HER2-advanced breast cancer who had progressed while receiving endocrine therapy. J Clin Oncol. 2017;35(25):2875–84.
7. Slamon DJ, Neven P, Chia SKL, Im S-A, Fasching PA, DeLaurentiis M, et al. Ribociclib (RIB) + fulvestrant (FUL) in postmenopausal women with hormone receptor-positive (HR+), HER2-negative (HER2–) advanced breast cancer (ABC): Results from MONALEESA-3. J Clin Oncol. 2018 May 20;36(15_suppl):1000.
8. Cristofanilli M, Turner NC, Bondarenko I, Ro J, Im SA, Masuda N, et al. Fulvestrant plus palbociclib versus fulvestrant plus placebo for treatment of hormone-receptor-positive, HER2-negative metastatic breast cancer that progressed on previous endocrine therapy (PALOMA-3): final analysis of the multicentre, double-blind, phas. Lancet Oncol. 2016;17(4):425–39.
9. Álvarez-Fernández M, Malumbres M. Mechanisms of Sensitivity and Resistance to CDK4/6 Inhibition. Cancer Cell. 2020 Apr;37(4):514–29.
10. Cejuela M, Gil-Torralvo A, Castilla MÁ, Domínguez-Cejudo MÁ, Falcón A, Benavent M, et al. Abemaciclib, Palbociclib, and Ribociclib in Real-World Data: A Direct Comparison of First-Line Treatment for Endocrine-Receptor-Positive Metastatic Breast Cancer. Int J Mol Sci. 2023 May 9;24(10):8488.
11. Keenan TE, Guerriero JL, Barroso-Sousa R, Li T, O'Meara T, Giobbie-Hurder A, et al. Molecular correlates of response to eribulin and pembrolizumab in hormone receptor-positive metastatic breast cancer. Nat Commun. 2021 Sep;12(1):5563.
12. Voorwerk L, Sanders J, Keusters MS, Balduzzi S, Cornelissen S, Duijst M, et al. Immune landscape of breast tumors with low and intermediate estrogen receptor expression. NPJ breast cancer. 2023 May;9(1):39.

13. Palomeque JÁ, Serra-Mir G, Blasco-Benito S, Brunel H, Torren-Duran P, Pérez-Núñez I, et al. Estrogen receptor signaling drives immune evasion and immunotherapy resistance in HR+ breast cancer. J Clin Invest. 2026 Jan;136(2).
14. Jeselsohn R, Yelensky R, Buchwalter G, Frampton G, Meric-Bernstam F, Gonzalez-Angulo AM, et al. Emergence of constitutively active estrogen receptor-α mutations in pretreated advanced estrogen receptor-positive breast cancer. Clin cancer Res an Off J Am Assoc Cancer Res. 2014 Apr;20(7):1757–67.
15. Herrera-Abreu MT, Palafox M, Asghar U, Rivas MA, Cutts RJ, Garcia-Murillas I, et al. Early adaptation and acquired resistance to CDK4/6 inhibition in estrogen receptor-positive breast cancer. Cancer Res. 2016;76(8):2301–13.
16. Finn RS, Aleshin A, Slamon DJ. Targeting the cyclin-dependent kinases (CDK) 4/6 in estrogen receptor-positive breast cancers. Breast Cancer Res. 2016 Feb;18(1):17.
17. Razavi P, Chang MT, Xu G, Bandlamudi C, Ross DS, Vasan N, et al. The Genomic Landscape of Endocrine-Resistant Advanced Breast Cancers. Cancer Cell. 2018 Sep;34(3):427-438.e6.
18. Turner NC, Slamon DJ, Ro J, Bondarenko I, Im S-A, Masuda N, et al. Overall Survival with Palbociclib and Fulvestrant in Advanced Breast Cancer. N Engl J Med. 2018 Nov;379(20):1926–36.
19. Garcia-Murillas I, Schiavon G, Weigelt B, Ng C, Hrebien S, Cutts RJ, et al. Mutation tracking in circulating tumor DNA predicts relapse in early breast cancer. Sci Transl Med. 2015;7(302):302ra133-302ra133.
20. Schiavon G, Hrebien S, Garcia-Murillas I, Cutts RJ, Pearson A, Tarazona N, et al. Analysis of ESR1 mutation in circulating tumor DNA demonstrates evolution during therapy for metastatic breast cancer. Sci Transl Med. 2015;7(313):313ra182-313ra182.
21. Chandarlapaty S, Chen D, He W, Sung P, Samoila A, You D, et al. Prevalence of ESR1 Mutations in Cell-Free DNA and Outcomes in Metastatic Breast Cancer: A Secondary Analysis of the BOLERO-2 Clinical Trial. JAMA Oncol. 2016 Oct;2(10):1310–5.
22. Preethi KA, Selvakumar SC, Ross K, Jayaraman S, Tusubira D, Sekar D. Liquid biopsy: Exosomal microRNAs as novel diagnostic and prognostic biomarkers in cancer. Mol Cancer. 2022 Feb;21(1):54.
23. Wang Q, Yan T, Cheng X. Bubble Ticket Trip : Exploring the Mechanism of miRNA Sorting into Exosomes and Maintaining the Stability of Tumor Microenvironment. 2024;(December):13671–85.
24. Jiang S, Zhang H-W, Lu M-H, He X-H, Li Y, Gu H, et al. MicroRNA-155 Functions as an OncomiR in Breast Cancer by Targeting the Suppressor of Cytokine Signaling 1 Gene. Cancer Res. 2010 Apr 14;70(8):3119–27.
25. Mann M, Mehta A, Zhao JL, Lee K, Marinov GK, Garcia-Flores Y, et al. An NF-κB-microRNA regulatory network tunes macrophage inflammatory responses. Nat Commun. 2017;8(1):851.
26. Jiang S, Zhang L, Zhang H, Hu S, Lu M, Liang S, et al. A novel miR155/miR143 cascade controls glycolysis by regulating hexokinase 2 in breast cancer cells. EMBO J. 2012 Apr 18;31(8):1985–98.

27. Hu S, Zhu W, Zhang L-F, Pei M, Liu M-F. MicroRNA-155 broadly orchestrates inflammation-induced changes of microRNA expression in breast cancer. Cell Res. 2014;24(2):254–7.
28. Gardiner C, Di Vizio D, Sahoo S, Théry C, Witwer KW, Wauben M, et al. Techniques used for the isolation and characterization of extracellular vesicles: results of a worldwide survey. J Extracell vesicles. 2016;5:32945.
29. Livak KJ, Schmittgen TD. Analysis of relative gene expression data using real-time quantitative PCR and the 2(-Delta Delta C(T)) Method. Methods. 2001 Dec;25(4):402–8.
30. Zhou X, Mao Y, Zhu J, Meng F, Chen Q, Tao L, et al. TGF-β1 promotes colorectal cancer immune escape by elevating B7-H3 and B7-H4 via the miR-155/miR-143 axis. Oncotarget; Vol 7, No 41. 2016;
31. Bacci M, Giannoni E, Fearns A, Ribas R, Gao Q, Taddei ML, et al. miR-155 Drives Metabolic Reprogramming of ER+ Breast Cancer Cells Following Long-Term Estrogen Deprivation and Predicts Clinical Response to Aromatase Inhibitors. Cancer Res. 2016 Mar 14;76(6):1615–26.
32. Kim S, Lee E, Jung J, Lee JW, Kim HJ, Kim J, et al. MicroRNA-155 positively regulates glucose metabolism via PIK3R1-FOXO3a-cMYC axis in breast cancer. Oncogene. 2018 May 1;37(22):2982–91.
33. Joshi T, Elias D, Stenvang J, Alves CL, Teng F, Lyng MB, et al. Integrative analysis of miRNA and gene expression reveals regulatory networks in tamoxifen-resistant breast cancer. Oncotarget. 2016 Aug;7(35):57239–53.
34. Martínez-Sáez O, Pascual T, Brasó-Maristany F, Chic N, González-Farré B, Sanfeliu E, et al. Circulating tumor DNA dynamics in advanced breast cancer treated with CDK4/6 inhibition and endocrine therapy. npj Breast Cancer. 2021;7(1):8.

Figures

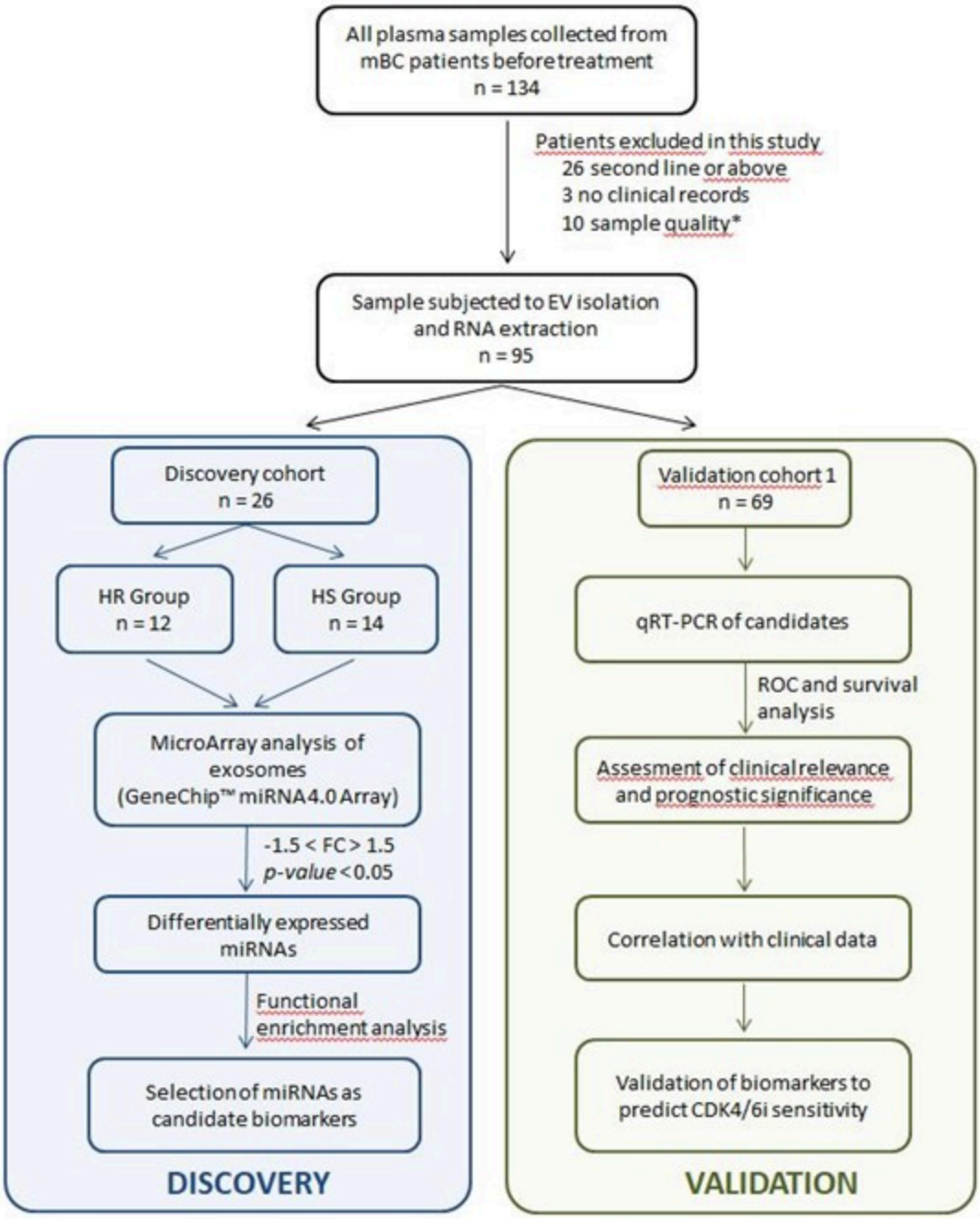


Figure 1

Legend not included with this version

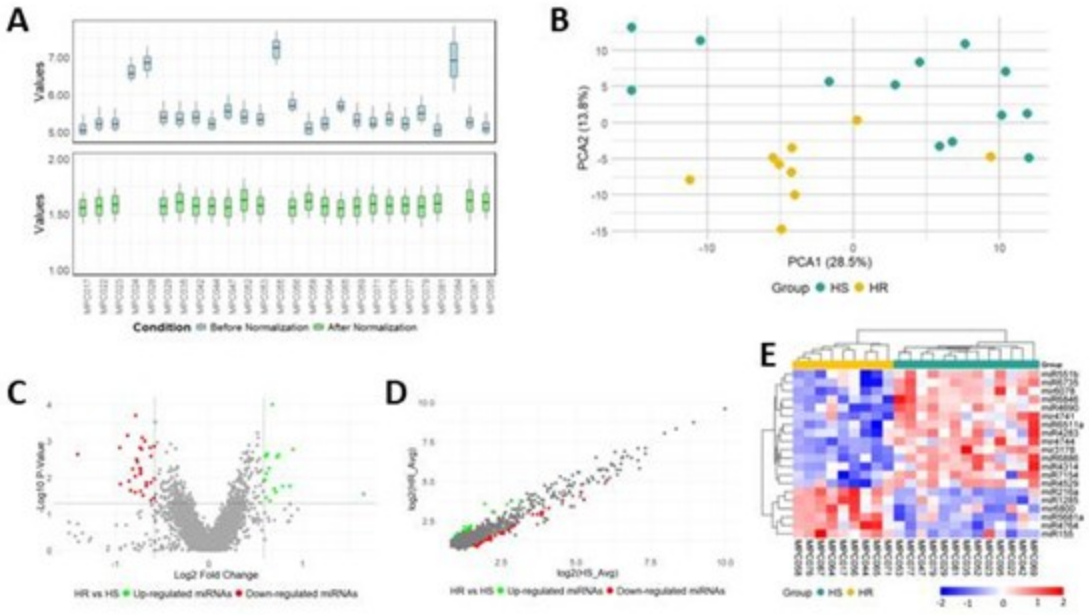


Figure 2

Identification of Candidate Biomarkers in the Exploratory Cohort.

A. Boxplot of the overall signal per sample before (upper panel) and after (lower panel) normalization. **B.** PCA to represent the distribution of samples according to their miRNA expression profile and the divergence between them. HS: hormone-sensitive; HR: hormone-resistant. **C.** Volcano plot and **D.**Scatter plot of miRNAs that are upregulated and downregulated in patient samples. Fold Change +/- 1.5; p-value <0,05. **E.** Heat map of the unsupervised hierarchical clustering analysis of the top 20 differentially expressed miRNAs.

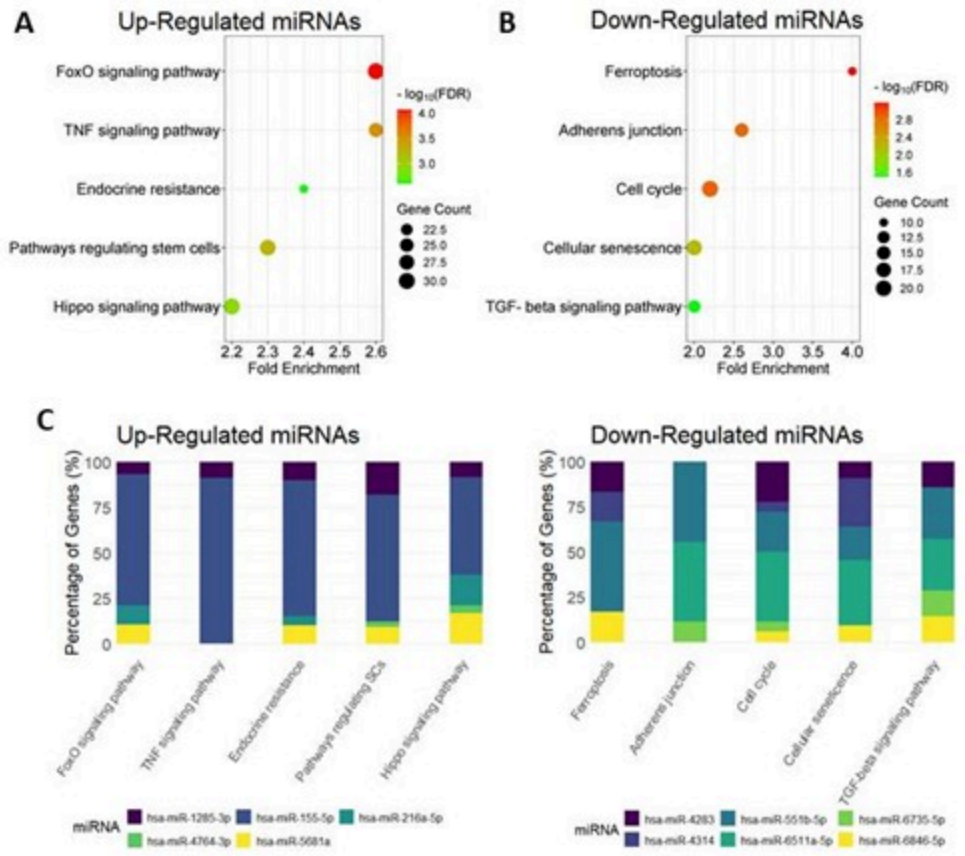


Figure 3

Functional Significance of Dysregulated miRNAs

A & B. Bubble plot for Kyoto Encyclopedia of Genes and Genomes (KEGG) pathway enrichment analysis of Up-regulated miRNAs (A) or down-regulated miRNAs (B). The y-axis shows pathway terms, whereas the x-axis denotes gene ratio. The color scale indicates different thresholds of the false discovery rate (FDR), and the size of the dot indicates the number of genes corresponding to each pathway. **C.** Relative contribution of individual miRNAs to each enriched pathway, shown as the percentage of target genes regulated by each miRNA within the corresponding pathway, for up-regulated (left) and down-regulated (right) miRNAs.

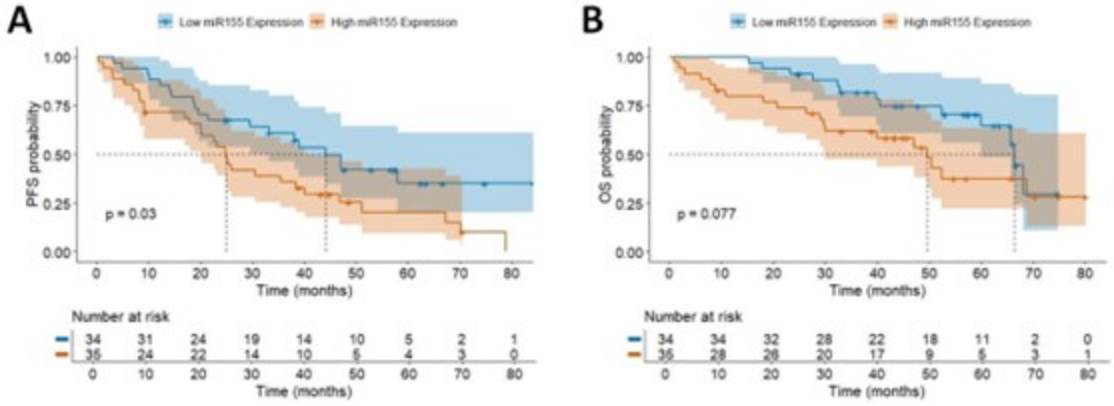


Figure 4

Validation of miR-155-5p as biomarker for Predicting Sensitivity to CDK4/6i therapy

A&B. Kaplan–Meier analysis of PFS (A) or OS (B) stratified by median exosomal miR-155-5p expression (high vs. low) in the validation cohort (n=69). Patients with high miR-155-5p levels exhibited significantly shorter PFS and OS compared with those with low miR-155-5p expression (log-rank p = 0.03 and 0.07, respectively). Shaded areas represent 95% confidence intervals, and the number of patients at risk at each time point is shown below the plot.

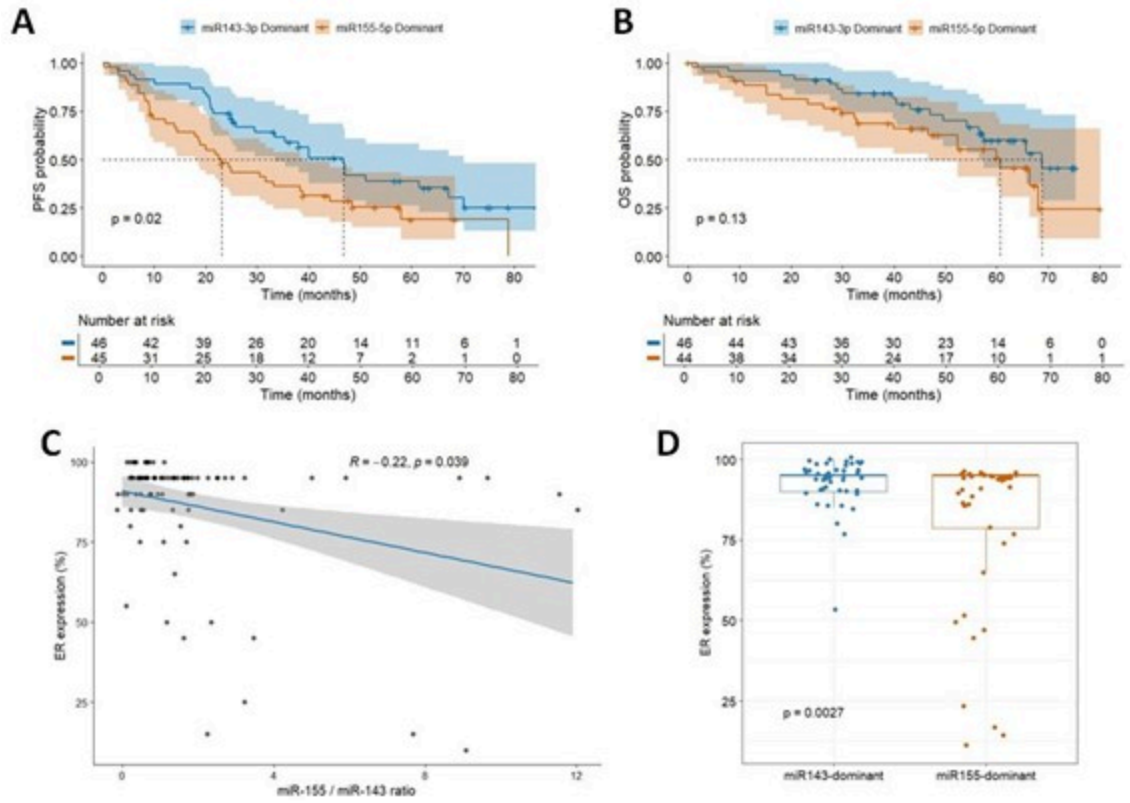


Figure 5

miR-155-5p is associated with inflammation, estrogen receptor expression, and treatment response. **A–B.** Kaplan–Meier analysis of PFS) (A) and overall survival (OS) (B) stratified by miRNA dominance based on the miR-155-5p/miR-143-3p expression ratio in the combined discovery and validation cohorts (n = 91). Patients with miR-155-dominant profiles exhibited significantly shorter PFS and a trend toward poorer OS compared with miR-143-dominant cases (log-rank p = 0.02 and p = 0.10, respectively). Shaded areas represent 95% confidence intervals, and the number of patients at risk at each time point is shown below the plots. **C.** Scatter plot showing the inverse correlation between estrogen receptor (ER) expression levels and the miR-155-5p/miR-143-3p ratio (Spearman ρ = −0.22, p = 0.038), indicating that higher relative miR-155-5p abundance is associated with lower ER expression. The solid line represents the fitted regression trend with 95% confidence band. **D.** Boxplot illustrating ER expression according to miRNA dominance groups. Tumors classified as miR-155-dominant displayed significantly lower ER

levels compared with miR-143-dominant tumors (Wilcoxon rank-sum test p = 0.0027). Boxes indicate median and interquartile range, with whiskers representing the full data distribution excluding outliers.

Supplementary Files

This is a list of supplementary files associated with this preprint. Click to download.

- SupTable3.docx
- SupFile.pdf
- SupFigures.pdf